

Net charge fluctuations and local charge compensation

Jinghua Fu*

Institute of Particle Physics, Huazhong Normal University, Wuhan 430079, People's Republic of China
(Received 8 October 2006; revised manuscript received 17 November 2006; published 22 December 2006)

We propose net charge fluctuation as a measure of local charge correlation length. It is demonstrated that, in terms of a schematic multiperipheral model, net charge fluctuation satisfies the same Quigg-Thomas relation as satisfied by charge transfer fluctuation. Net charge fluctuations measured in finite rapidity windows depend on both the local charge correlation length and the size of the observation window. When the observation window is larger than the local charge correlation length, the net charge fluctuation only depends on the local charge correlation length, while forward-backward charge fluctuations always have strong dependence on the observation window size. Net charge fluctuations and forward-backward charge fluctuations measured in the present heavy ion experiments show characteristic features similar to those from multiperipheral models. But the data cannot all be understood within this simple model.

DOI: [10.1103/PhysRevC.74.064912](https://doi.org/10.1103/PhysRevC.74.064912)

PACS number(s): 24.60.Ky, 25.75.Gz, 13.85.Hd

I. INTRODUCTION

Particle correlation in longitudinal phase space, i.e., two-particle rapidity correlation, has been well studied in low-energy hadron-hadron collisions [1,2]. Strong short-range correlations over a region of ± 1 unit in rapidity were observed. These short-range correlations can be understood in terms of a model in which low-mass clusters decay into a small number of charged and neutral pions. An interesting possibility is that the clusters have the same properties in all reactions at all energies. This possibility is in the spirit of the multiperipheral models, but it is certainly not the only possibility. Multiperipheral models obey the local compensation of quantum numbers [3]. An additive quantum number Q is said to be locally compensated if each particle carrying the value q is almost always surrounded by a small number of particles in the neighboring region of rapidity space carrying a total quantum number of $-q$ [4,5]. The STAR experiment at BNL's Relativistic Heavy Ion Collider (RHIC) measured charge particle angular correlation and suggested local charge conservation during hadronization in heavy ion collisions as in pp collisions [6]. Other theoretical investigations suggested that two-particle correlation in ultrarelativistic heavy ion collisions might be significantly altered because of the formation of quark gluon plasma (QGP) [7]. It would be interesting to test whether this local conservation of charge is still valid in heavy ion collisions and compare it with the corresponding pp collisions.

Net charge in a rapidity region $y_i \in [y_a, y_b]$, $y_a < y_b$, can be defined as

$$Q(y_a, y_b) = \sum_i q_i \theta(y_i - y_a) \theta(y_b - y_i), \quad (1)$$

where q_i is the charge of particle i and $\theta(x)$ is the step function defined as usual by $\theta(x) = 1$, if $x \geq 0$, and $\theta(x) = 0$, if $x < 0$. The reduction of the fluctuation of net charge

$$\sigma^2(Q) = \langle Q^2 \rangle - \langle Q \rangle^2 \quad (2)$$

has been suggested as a signal of the formation of the QGP state because the charge carriers in the plasma state carry less charge than that in ordinary hadronic state [8,9]. Available experimental investigations of net charge fluctuations [10,11] show no indication of the QGP state, and the results are consistent with resonance gases. In this paper, we will demonstrate that the measure of net charge fluctuation could also be used as a test of local conservation of charge and as a measure of the local charge correlation length.

We study net charge fluctuations in terms of a schematic multiperipheral model in Sec. II. In Sec. III, modifications on the results from Sec. II due to limited rapidity coverage are studied. Section IV discusses the STAR experiment results on net charge fluctuations and compares them with our model studies. In Sec. V, a related measurement, forward-backward charge fluctuation, is discussed briefly. A summary is given in Sec. VI.

II. NET CHARGE FLUCTUATION IN A MULTIPERIPHERAL PICTURE

Quigg and Thomas studied charge transfer fluctuations in a schematic multiperipheral model [12]. The charge transfer is defined as

$$u(y) = [Q_F(y) - Q_B(y)]/2, \quad (3)$$

where $Q_B(y) = \sum_i q_i \theta(y - y_i)$ is the net charge in the rapidity region backward of y . Similarly, $Q_F(y) = \sum_i q_i \theta(y_i - y)$ is the net charge in the rapidity region forward of y . It is assumed that the full rapidity range is measured. An “ ω ” model was used as an example to study charge transfer fluctuations in their original paper. In that model, pions are produced in a basic cluster of triplets ($\pi^+ \pi^- \pi^0$) for which a cluster produced at rapidity y_i will yield pions at rapidities $y_i - \Delta$, y_i , and $y_i + \Delta$. Δ is a “mobility” parameter which characterizes the emergence of pions from a cluster. It is assumed that the clusters are produced independently with a flat rapidity distribution. It is easy to see that only those clusters with rapidities within the interval $[y - \Delta, y + \Delta]$ have the potential to contribute

*Electronic address: fujh@iopp.cnu.edu.cn

to $u(y)$. The central result they obtained on charge transfer fluctuation is

$$\sigma^2(u(y)) = \langle u(y)^2 \rangle - \langle u(y) \rangle^2 = \frac{2}{3} 2\Delta \frac{N}{Y}, \quad (4)$$

in which N is the number of clusters produced in the rapidity interval $[-Y/2, Y/2]$ in an event. This result was later extended by Chao and Quigg [13] to yield the smooth rapidity distribution

$$\sigma^2(u(y)) = \kappa \frac{dn_{ch}}{dy}, \quad (5)$$

where dn_{ch}/dy is the charged particle density after elimination of the leading particles. The proportion coefficient κ is determined by the mobility parameter Δ in the cluster model and directly related to the local charge correlation length. The Quigg-Thomas relation has been observed in low-energy pp collisions, and κ is found to remain nearly constant with rapidity [14]. These results can be taken as an indication of local compensation of charge in hadron-hadron collisions.

In terms of the ω model, $Q_B(y) = -Q_F(y)$ is satisfied for every event. From the definition of charge transfer, we have $u(y) = Q_F(y) = -Q_B(y)$. All the derivations in Ref. [12] for charge transfer fluctuation $\sigma^2(u(y))$ are valid for the net charge fluctuation $\sigma^2(Q_B(y))$ [or $\sigma^2(Q_F(y))$], and these lead to

$$\sigma^2(Q_B(y)) = \sigma^2(Q_F(y)) = \sigma^2(u(y)) = \kappa \frac{dn_{ch}}{dy}. \quad (6)$$

To examine the above relation, we analyzed 1 000 000 HIJING-simulated [15] 200-GeV pp collision events. The results of $\sigma^2(Q_B(y))$ as a function of rapidity are shown in Fig. 1. Since $\sigma^2(Q_B(y))$ and $\sigma^2(Q_F(y))$ are the same, we only show the results for $\sigma^2(Q_B(y))$. Also shown in the figure are $\sigma^2(u(y))$ and scaled dn_{ch}/dy . Indeed, we see that net charge fluctuations $\sigma^2(Q_B(y))$ and charge transfer fluctuations $\sigma^2(u(y))$ as a function of rapidity y are identical. The Quigg-Thomas relation is fulfilled for both $\sigma^2(u(y))$ and $\sigma^2(Q_B(y))$ in the HIJING simulation. The proportion

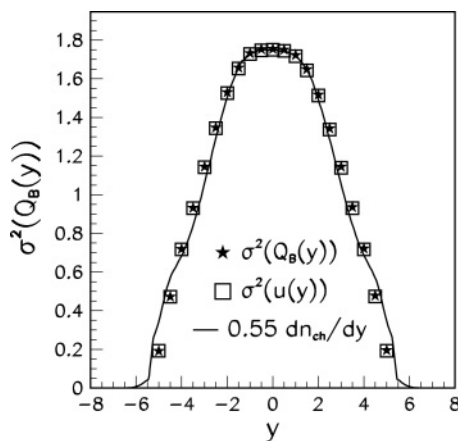


FIG. 1. Net charge fluctuations as a function of rapidity (stars) compared with charge transfer fluctuations (open squares) and charged particle rapidity distribution scaled by a factor of 0.55 (line). The results are from 1 000 000 HIJING-simulated 200-GeV pp collision events.

coefficient $\kappa \approx 0.55$, and it remains nearly constant with change in rapidity.

In the above discussion, it was assumed that the effects of the leading particles are eliminated. This is approximately true in the central rapidity region for RHIC heavy ion collisions [16]. In this paper, we will concentrate on the study of net charge fluctuations. A detailed analysis of charge transfer fluctuations is available in Ref. [17].

Equation (6) indicates that if there is clustering in many-particle production, the net charge fluctuation depends on the charged particle density dn_{ch}/dy . In a stochastic scenario of independent emission, as we already know, net charge fluctuation depends on the total charged multiplicity $\sigma^2(Q) = n_{ch}$. We might take these as two limiting cases. If particles are produced independently, then $\sigma^2(Q)/n_{ch}$ is a constant. If particles are produced through clusters, then $\sigma^2(Q)/(dn_{ch}/dy)$ is a constant (assuming the same cluster everywhere) while $\sigma^2(Q)/n_{ch}$ will decrease with the increase of the rapidity range; see, for example, Figs. 1(a) and 1(d) in Ref. [18].

III. NET CHARGE FLUCTUATION IN LIMITED RAPIDITY REGIONS

In Sec. II, we assumed that the complete rapidity range could be measured. This is generally not the case for current heavy ion experiments. Most of the detectors only have a coverage in central rapidity. It would be interesting to study how the results for net charge fluctuation in a multiperipheral picture would change when the observation is made in a finite rapidity window. An example of the configuration is depicted in Fig. 2 to help us visualize the construction of the generating functions $P_N(x)$, where N is the number of clusters produced in an event and x is a dummy parameter [12]. Particles are emitted in full rapidity range $[-Y/2, Y/2]$, while the observation is made in the rapidity window $[y_a, y_b]$. In this case, $Q_B(y_a, y)$ is defined as $Q_B(y_a, y) = \sum_i q_i \theta(y_i - y_a) \theta(y - y_i)$, and from now on we will just write it as $Q(y_a, y)$.

Similar to Ref. [12], we consider the simple ω model. Clusters are produced independently with flat rapidity distribution. If the detector has a full coverage over $[-Y/2, Y/2]$, only those clusters with rapidities lying in $(-\Delta, \Delta)$ around y have the possibility of contributing to $Q(y)$, as discussed in Sec. II. Clusters emitted in the interval $[-Y/2, y - \Delta]$ will deposit all their charged secondaries in the region left of y , and their charges add up to zero. If the measurement is limited to $[y_a, y_b]$, clusters emitted around y_a might deposit part of their charged secondaries inside $[y_a, y]$ and part of them outside $[y_a, y]$ and gain the potential to contribute to $Q(y_a, y)$. How the clusters produced around y and y_a will affect $Q(y_a, y)$ depends on how far away y is from y_a . Let us say $y - y_a = \delta y$.

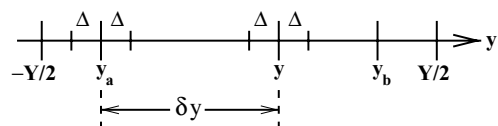


FIG. 2. Center-of-mass system rapidity observation window used in the analysis of net charge fluctuations.

TABLE I. Net charge fluctuation from ω model for different sizes of rapidity observation window.

$\delta y = y - y_a$	Generating function $P_N(x)$	$\sigma^2(Q(y, y_a)) = \sigma^2(Q(\delta y))$
$\delta y \leq \Delta$	$[(1 - 3\frac{\delta y}{Y}) + \frac{\delta y}{Y}(x + 1 + x^{-1})]^N$	$2\delta y \frac{N}{Y}$
$\Delta < \delta y < 2\Delta$	$[(1 - \frac{\delta y + 2\Delta}{Y}) + \frac{1}{3}\frac{\delta y + 2\Delta}{Y}(x + 1 + x^{-1})]^N$	$\frac{2}{3}(\delta y + 2\Delta) \frac{N}{Y}$
$\delta y \geq 2\Delta$	$[(1 - 4\frac{\Delta}{Y}) + \frac{4}{3}\frac{\Delta}{Y}(x + 1 + x^{-1})]^N$	$\frac{2}{3}(2\Delta + 2\Delta) \frac{N}{Y}$

If $\delta y > 2\Delta$, as sketched in Fig. 2, clusters emitted in both $[y - \Delta, y + \Delta]$ and $[y_a - \Delta, y_a + \Delta]$ have the possibility of contributing to $Q(y_a, y)$. In this case, the clusters emitted in the intervals $[y - \Delta, y + \Delta]$ and $[y_a - \Delta, y_a + \Delta]$ are called “active.” Depending on the distance δy between y and y_a , the intervals for active clusters might be different, which makes the generating function different. Clusters emitted in $[y + \Delta, Y/2]$ are not relevant to the measurement of $Q(y_a, y)$. With the foregoing analysis, one could readily write down the generating function for different values of δy . The results are listed in Table I, together with the resultant $\sigma^2(Q(y_a, y))$.

Since only charged particles in the region $[y_a, y]$ are counted in the measurement of $Q(y_a, y)$, we will call $[y_a, y]$ the observation window, and δy is the size of the observation window. Some characteristic features from the results in Table I are noteworthy, and they are more general than the special implementation of the ω model. First, net charge fluctuation measured in a finite rapidity window depends on the charged particle density dn_{ch}/dy as that measured in the full rapidity region. Second, when $\delta y \leq \Delta$, the net charge fluctuation divided by $dn_{ch}/d\eta$ depends only on δy , the size of the observation window; when $\Delta < \delta y < 2\Delta$, it depends on both δy and the cluster model mobility parameter Δ ; when $\delta y \geq 2\Delta$, it only depends on Δ . These features lead to the observation that if all the clusters have the same Δ , as assumed in multiperipheral models, the net charge fluctuation divided by $dn_{ch}/d\eta$ will first increase with the increase of δy and then saturate when $\delta y \geq 2\Delta$ at a value which is two times that when no rapidity cut is implemented [cf. Eq. (4)]. Notice, although net charge fluctuation and charge transfer fluctuation in the ω model are identical when the whole rapidity range is measured, their behavior in finite rapidity windows could be quite different [19], because clusters emitted in the interval $[y + \Delta, Y/2]$ need to be included in the calculation of charge transfer fluctuation. In this sense, net charge fluctuation keeps the property of charge transfer fluctuation and simplifies the calculation.

All the arguments above do not depend on the phase space variable we used. For an easy comparison with experiment, we will exclusively use pseudorapidity in the following analysis.

Again we use HIJING 200 GeV pp collision simulations to see if these features obtained from model analysis could be observed there; the results are shown in Fig. 3.

We assumed three cases of detector coverage in pseudorapidity as $[-2.2, 2.2]$, $[-1.6, 1.6]$, and $[-1.0, 1.0]$, and the measurements are made at η s with 0.2 intervals in each case. $\sigma^2(Q(y_a, y))/(dn_{ch}/d\eta)$ is now simply written as $\sigma^2(Q)/(dn_{ch}/d\eta)$. For all three cases, $\sigma^2(Q)/(dn_{ch}/d\eta)$ first increases with the increase of observation window size $\delta\eta$ and starts to saturate when the observation window size

$\delta\eta$ is about 2 units of pseudorapidity, consistent with what we obtained from the ω model analysis. The saturating value of $\sigma^2(Q)/(dn_{ch}/d\eta)$ is about two times the $\kappa(=0.55)$ measured in Sec. II from the same simulation. When $\delta\eta$ is the same, the resulting $\sigma^2(Q)/(dn_{ch}/d\eta)$ values almost do not depend on how we choose the detector coverage. The measured results from three different coverages are almost parallel to each other. This feature can be observed more clearly in Fig. 4, where the observations are made at $\eta = -1.5, -0.5, 0.5, \text{ and } 1.5$, and the observation windows at each η are chosen as $[\eta - \delta\eta/2, \eta + \delta\eta/2]$ with $\delta\eta = 0.2, 0.4, 0.6, 0.8, \text{ and } 1.0$. The results indicate that when $\delta\eta$ is the same, $\sigma^2(Q)/(dn_{ch}/d\eta)$ almost does not change with η , especially when $\delta\eta$ is small. According to Table I, this is because $\sigma^2(Q)/(dn_{ch}/d\eta)$ depends only on $\delta\eta$ and Δ . When $\delta\eta$ is same, $\sigma^2(Q)/(dn_{ch}/d\eta)$ does not change with η , which means that the local charge correlation length does not change with η . A measure of net charge fluctuation can therefore be used as a measure of local charge correlation length.

IV. NET CHARGE FLUCTUATIONS IN RELATIVISTIC HEAVY ION COLLISIONS

Net charge fluctuations have been measured in a couple of relativistic heavy ion collision experiments [10,11]. Because of the limited rapidity coverage of detectors, they are all measured in finite rapidity windows. The STAR experiment

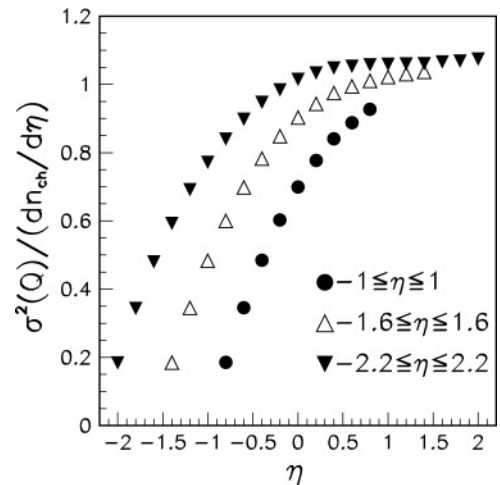


FIG. 3. Net charge fluctuation divided by $dn_{ch}/d\eta$ for different pseudorapidity coverage chosen as $[-2.2, 2.2]$ (full triangles), $[-1.6, 1.6]$ (open triangles), and $[-1.0, 1.0]$ (full dots). The measurements are made at η s with 0.2 intervals in each case.

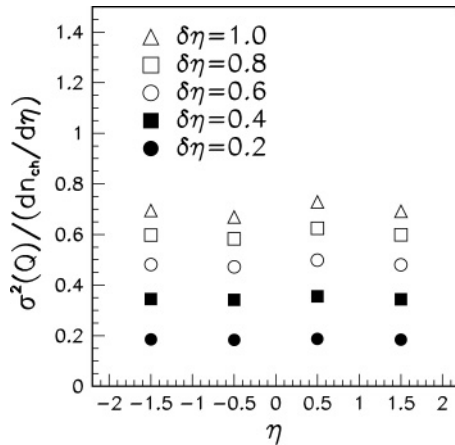


FIG. 4. Net charge fluctuations divided by $dn_{ch}/d\eta$ for different pseudorapidity observation windows as a function of pseudorapidity. Observations were made at $\eta = -1.5, -0.5, 0.5,$ and 1.5 ; observation windows at each η were chosen as $[\eta - \delta\eta/2, \eta + \delta\eta/2]$, with the $\delta\eta$ values as shown in figure.

at RHIC has measured net charge fluctuation as a function of the pseudorapidity range [10]. In their original paper, they measured $\nu_{+-,\text{dyn}}$. We convert it to $\sigma^2(Q)$ with the formula $\frac{\sigma^2(Q)}{(n_{ch})} \approx 1 + \frac{1}{4}(n_{ch})\nu_{+-,\text{dyn}}$ [20], and the results are shown in Fig. 5 (stars). Charged particle density used in the conversion are from Ref. [21]. Ten pseudorapidity ranges are measured from a minimal $-0.1 < \eta < 0.1$ to a maximal $-1 < \eta < 1$ in discrete steps of 0.1 units of pseudorapidity.

We made the same measurement with HIJING simulations while extending the observation windows to $-2 < \eta < 2$ in the same manner. The results for 130-GeV HIJING Au-Au collisions are indicated as open circles in Fig. 5; the results from 130-GeV HIJING pp collisions as open triangles. Errors

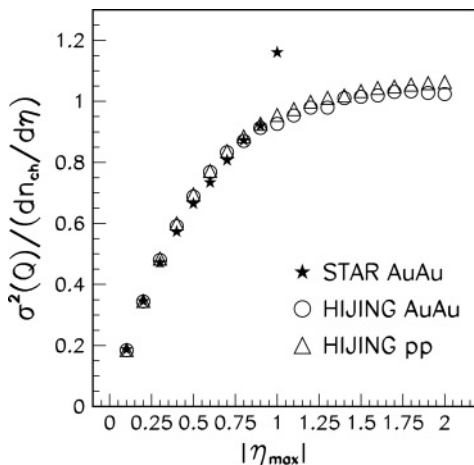


FIG. 5. Net charge fluctuations divided by $dn_{ch}/d\eta$ as a function of pseudorapidity range from STAR experiment compared with those from HIJING Au-Au and pp collisions. For STAR data, the pseudorapidity ranges are $-0.1 < \eta < 0.1$ to $-1 < \eta < 1$ in discrete steps of 0.1 units of pseudorapidity. For HIJING simulations, the pseudorapidity ranges are chosen in the same way but extended to $-2 < \eta < 2$.

for STAR data are not included. For the HIJING simulation, errors are within the data points. The HIJING Au-Au and pp collision results are quite similar. The STAR data points for $\sigma^2(Q)/(dn_{ch}/d\eta)$ increase with the pseudorapidity range as expected from the multiperipheral model, and most of them can be described by HIJING simulations except the last point for $-1 < \eta < 1$. The STAR data show a sudden increase at $-1 < \eta < 1$, far beyond that of the previous point at $-0.9 < \eta < 0.9$, while HIJING results start to saturate around $-1 < \eta < 1$. Since only one point from experiment cannot be explained consistently within the model, further investigations are needed to understand why the last STAR data point does not follow the saturation trend and to make a conclusion on what this discrepancy implies, whether it comes from the onset of different correlation length or from long-range correlations or is caused by some other dynamics.

In the same paper [10], STAR also measured $\nu_{+-,\text{dyn}}$ as a function of collision centrality in $|\eta| \leq 0.5$. The event sample is divided into eight centrality classes based on the fraction of triggered events: 6%, 11%, 18%, 26%, 34%, 45%, 58%, and 84%. The converted results for $\sigma^2(Q)/(dn_{ch}/d\eta)$ are plotted in Fig. 6 together with the HIJING simulation results for 130-GeV Au-Au collisions. Class 1 in the figure represents the most central events. The STAR data show a decrease of $\sigma^2(Q)/(dn_{ch}/d\eta)$ from peripheral to central. In view of cluster models, because the pseudorapidity intervals are all the same, this decrease means a slight decrease of local charge correlation length from peripheral to central. It is consistent with the balance function measurement from the same experiment [22]. HIJING simulation results show much less dependence on centrality.

PHENIX experiment at RHIC measured net charge fluctuation as a function of collision centrality in $|\eta| < 0.35$ and found it to be almost flat [11] within errors. A higher statistics measurement will provide us with a better understanding of the dependence of net charge fluctuations on centrality.

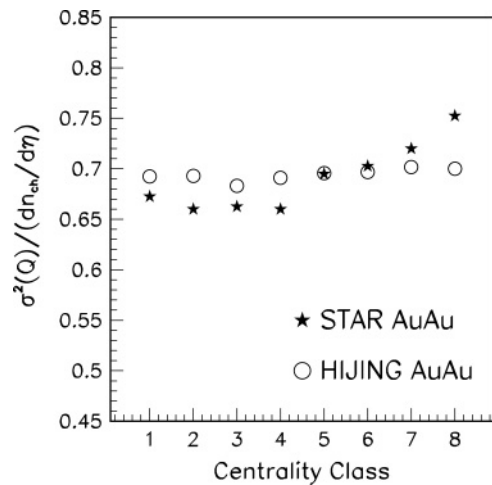


FIG. 6. Net charge fluctuation measured in $|\eta| \leq 0.5$ as a function of the collision centrality from STAR experiment (stars) and HIJING 130-GeV Au-Au simulation (open circles).

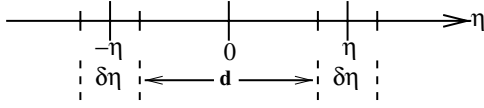


FIG. 7. Forward and backward pseudorapidity intervals.

V. FORWARD-BACKWARD CHARGE FLUCTUATIONS

Recently, a related measurement of forward-backward charge fluctuations was made by the PHOBOS experiment at RHIC for Au+Au collisions at $\sqrt{s_{NN}} = 200$ GeV [23]. They defined an eventwise variable $C = \frac{n_F - n_B}{\sqrt{n_F + n_B}}$, where n_F and n_B are the number of charged particles in two symmetric pseudorapidity intervals centered at $\pm\eta$ with equal width $\delta\eta$, as depicted in Fig. 7. They measured the variance σ_C^2 for both central and peripheral collisions.

The η and $\delta\eta$ dependence of forward-backward charge fluctuations could also be estimated in a multiperipheral picture. To simplify the derivation, we chose an even simpler “ ρ ” model in which a cluster produced with pseudorapidity η results in $\pi^+\pi^-$ at $\eta \pm \Delta$. None of the qualitative conclusions we wish to draw depends on this special implementation of the model. How a cluster deposits its charged secondaries depends on the pseudorapidity of the cluster and the position and size of the forward and backward pseudorapidity intervals. The results of the generating function $P_N(x)$ and $\sigma^2(n_F - n_B)$ for different situations are listed in Table II, where N is the number of clusters produced in an event and Y is the full (pseudo)rapidity interval width for particle production. For the model we used, there are six possible situations with increasing size of $\delta\eta$ and d , where d is the distance between the upper edge of the backward interval and the lower edge of the forward interval, as depicted in Fig. 7.

The results indicate that, similar to net charge fluctuation, forward-backward charge fluctuation depends on the charged particle density $\frac{N}{Y}$ or $\frac{dn_{ch}}{d\eta}$. When the largest separation between the forward and backward intervals is less than the local charge correlation length, which is case 1 in the table, the forward-backward charge fluctuation is determined by only the forward and backward bin width $\delta\eta$. As the bin size $\delta\eta$ increases or their separation d increases, a cluster might deposit one of its charged secondaries in the forward bin and the other in the backward bin, and their

contributions to $n_F - n_B$ add up to zero. These correspond to cases 2 and 3 in the table, where clustering reduces the fluctuations. In case 4, the separation between the forward and backward bins increases even farther to larger than the typical charge correlation length, and the forward-backward charge fluctuations become dependent only on the bin size again. In the model we used, local charge correlation is assumed to have a fixed correlation length 2Δ . In the real situation, short-range correlations between charged particles as a function of their pseudorapidity differences are believed to have a continuous (exponential) distribution. For these reasons, when we fix the forward and backward bin sizes and measure the η dependence of $\sigma^2(n_F - n_B)/(dn_{ch}/d\eta)$, we observe the first few points to be lower, because the short-range correlation reduces the fluctuation; and when d becomes larger than the charge correlation length, $\sigma^2(n_F - n_B)/(dn_{ch}/d\eta)$ saturates at a constant value determined by the bin size $\delta\eta$. Cases 5 and 6 in the table are for forward and backward bin sizes larger than the typical charge correlation length. In these cases, two charged particles from one cluster might fall into the same forward or backward bin together, which makes the forward-backward charge fluctuations have an even stronger dependence on the bin size (larger coefficient in front of $\delta\eta$). To summarize, in a multiperipheral picture, forward-backward charge fluctuations have strong dependence on the forward and backward bin size. When the bin size is the same and the separation between the two bins is not too small, $\sigma^2(n_F - n_B)/(dn_{ch}/d\eta)$ should be approximately the same. When the forward and backward bin size increases, $\sigma^2(n_F - n_B)/(dn_{ch}/d\eta)$ increases linearly with the bin size. Compared with net charge fluctuations, forward-backward charge fluctuations are more controlled by the forward and backward window size than by the local charge correlation length. These features are understandable because only clusters on the border contribute to net charge fluctuations, while clusters depositing in the whole observation window contribute to forward-backward charge fluctuations.

The PHOBOS experiment reported the η dependence of σ_C^2 for $\delta\eta = 0.5$ units wide forward and backward bins and the $\delta\eta$ dependence of σ_C^2 for a fixed bin center position $\eta = 2.0$. The PHOBOS results do indicate σ_C^2 increases linearly with the forward and backward bin size $\delta\eta$. When the bin size is fixed, the PHOBOS results from central collisions do not change with η except for the first point, which is understandably

TABLE II. Forward-backward charge fluctuations from ρ model for different positions and sizes of forward and backward pseudorapidity intervals.

	$\delta\eta, d$	Generating function $P_N(x)$	$\sigma^2(n_F - n_B)$
Case 1	$2\delta\eta + d \leq 2\Delta$	$[(1 - 4\frac{\delta\eta}{Y}) + 2\frac{\delta\eta}{Y}(x + x^{-1})]^N$	$4\delta\eta\frac{N}{Y}$
Case 2	$2\delta\eta + d > 2\Delta,$ $\delta\eta + d \leq 2\Delta$	$[(1 - 4\frac{\Delta}{Y} + 2\frac{d}{Y}) + (2\frac{\Delta}{Y} - \frac{d}{Y})(x + x^{-1})]^N$	$(4\Delta - 2d)\frac{N}{Y}$
Case 3	$\delta\eta + d > 2\Delta,$ $\delta\eta \leq 2\Delta, d \leq 2\Delta$	$[(1 + 4\frac{\Delta}{Y} - 4\frac{\delta\eta}{Y} - 2\frac{d}{Y}) + (2\frac{\delta\eta}{Y} + \frac{d}{Y} - 2\frac{\Delta}{Y})(x + x^{-1})]^N$	$(4\delta\eta + 2d - 4\Delta)\frac{N}{Y}$
Case 4	$\delta\eta \leq 2\Delta, d > 2\Delta$	$[(1 - 4\frac{\delta\eta}{Y}) + 2\frac{\delta\eta}{Y}(x + x^{-1})]^N$	$4\delta\eta\frac{N}{Y}$
Case 5	$\delta\eta > 2\Delta, d \leq 2\Delta$	$[(1 - 2\frac{\delta\eta}{Y} - 2\frac{d}{Y}) + (2\frac{\Delta}{Y} + \frac{d}{Y})(x + x^{-1}) + (\frac{\delta\eta}{Y} - 2\frac{\Delta}{Y})(x^2 + x^{-2})]^N$	$(8\delta\eta + 2d - 12\Delta)\frac{N}{Y}$
Case 6	$\delta\eta > 2\Delta, d > 2\Delta$	$[(1 - 2\frac{\delta\eta}{Y} - 4\frac{\Delta}{Y}) + 4\frac{\Delta}{Y}(x + x^{-1}) + (\frac{\delta\eta}{Y} - 2\frac{\Delta}{Y})(x^2 + x^{-2})]^N$	$(8\delta\eta - 8\Delta)\frac{N}{Y}$

lower because short-range correlations reduce the fluctuations. The PHOBOS results from peripheral collisions for fixed bin size seem to not follow this trend. They keep on increasing with η , which cannot be explained within this model. Also, the PHOBOS results show a faster increase of forward-backward charge fluctuations with the increase of bin size in peripheral collisions than that seen in central collisions, which cannot be explained consistently in a multiperipheral picture either [24]. However, it should be mentioned that the best observable to compare with multiperipheral models is $\sigma^2(n_F - n_B)/(dn_{ch}/d\eta)$ which is not exactly the same as the σ_C^2 used in the PHOBOS experiment, and this might also cause some differences.

VI. SUMMARY

We demonstrated in this paper that, in terms of a schematic multiperipheral model, net charge fluctuation satisfies the same Quigg-Thomas relation as satisfied by charge transfer fluctuation. HIJING Monte Carlo simulation confirmed that when the measurements are made in full rapidity range, net charge fluctuation and charge transfer fluctuation are identical, and they both satisfy the Quigg-Thomas relation. We studied in detail the behavior of net charge fluctuation when the measurements are made in finite rapidity windows. In terms of the same ω model, net charge fluctuations in finite rapidity windows show some interesting characteristic features: (i) When the size $\delta\eta$ of the observation window is small, net charge fluctuation divided by charged particle density $dn_{ch}/d\eta$ will increase as the observation window size increases. (ii) Net charge fluctuation divided by $dn_{ch}/d\eta$ starts to saturate and depends only on the local charge correlation length when $\delta\eta$ increases to about two times the mobility parameter of

the cluster model. (iii) When $\delta\eta$ is the same, the net charge fluctuation divided by $dn_{ch}/d\eta$ depends only on the cluster model mobility parameter and can be used as a measure of local charge correlation length. HIJING simulation results qualitatively satisfy these features.

Most of the net charge fluctuation results from the STAR experiment can be explained in terms of the simple schematic multiperipheral model analysis and are consistent with HIJING simulations. No obvious change of local charge correlation length with pseudorapidity is observed within the STAR detector coverage except for the STAR result for $-1 < \eta < 1$, where an unexpected large increase of net charge fluctuation is observed. Further investigations are needed to understand its origin.

In terms of multiperipheral models, forward-backward charge fluctuations always have strong dependence on the forward and backward window size. PHOBOS results on forward-backward charge fluctuations show this window size dependence, but its results for both central and peripheral collisions cannot all be explained consistently within the model.

We suggest measuring net charge fluctuation as a function of pseudorapidity range and centrality to see if any sudden changes of local charge correlation length occur in ultrarelativistic heavy ion collisions.

ACKNOWLEDGMENTS

I would like to thank Prof. Wu Yuanfang for stimulating me to do this work and for her helpful discussions. This work was supported in part by the NSFC under Project No. 10305004 and by MOE of China under Project No. CFKSTIP-704035.

-
- [1] L. Foà, Phys. Rep. **22**, 1 (1975).
 - [2] G. J. Alner *et al.* (UA5 Collaboration), Phys. Rep. **154**, 247 (1987).
 - [3] M. Le Bellac, Yellow Report CERN 76-14, 1976 (unpublished).
 - [4] A. Krzywicki and D. Weingarten, Phys. Lett. **B50**, 265 (1974).
 - [5] D. Weingarten, Phys. Rev. D **11**, 1924 (1975).
 - [6] J. Adams *et al.* (STAR Collaboration), Phys. Lett. **B634**, 347 (2006).
 - [7] S. A. Bass, P. Danielewicz, and S. Pratt, Phys. Rev. Lett. **85**, 2689 (2000).
 - [8] S. Jeon and V. Koch, Phys. Rev. Lett. **85**, 2076 (2000).
 - [9] M. Asakawa, U. Heinz, and B. Müller, Phys. Rev. Lett. **85**, 2072 (2000).
 - [10] J. Adams *et al.* (STAR Collaboration), Phys. Rev. C **68**, 044905 (2003).
 - [11] K. Adcox *et al.* (PHENIX Collaboration), Phys. Rev. Lett. **89**, 082301 (2002).
 - [12] C. Quigg and G. H. Thomas, Phys. Rev. D **7**, 2752 (1973).
 - [13] A. W. Chao and C. Quigg, Phys. Rev. D **9**, 2016 (1974).
 - [14] T. Kafka *et al.*, Phys. Rev. Lett. **34**, 687 (1975).
 - [15] M. Gyulassy and X.-N. Wang, Comput. Phys. Commun. **83**, 307 (1994).
 - [16] C. Adler *et al.* (STAR Collaboration), Phys. Rev. Lett. **86**, 4778 (2001).
 - [17] L. Shi and S. Jeon, Phys. Rev. C **72**, 034904 (2005).
 - [18] M. R. Atayan *et al.* (NA22 Collaboration), Phys. Rev. D **71**, 012002 (2005).
 - [19] S. Jeon, L. Shi, and M. Bleicher, Phys. Rev. C **73**, 014905 (2006).
 - [20] C. Pruneau, S. Gavin, and S. Voloshin, Phys. Rev. C **66**, 044904 (2002).
 - [21] C. Adler *et al.* (STAR Collaboration), Phys. Rev. Lett. **87**, 112303 (2001).
 - [22] J. Adams *et al.* (STAR Collaboration), Phys. Rev. Lett. **90**, 172301 (2003).
 - [23] B. B. Back *et al.* (PHOBOS Collaboration), Phys. Rev. C **74**, 011901(R) (2006).
 - [24] Mohamed Abdel-Aziz and Marcus Bleicher, 2006, nucl-th/0605072.